ORQA

Houwink, Sietze G.; Kliffen, Klaas Y.; Kosinka, Jiri

Published in:
Proceedings of Computer Graphics & Visual Computing (CGVC) 2020

DOI:
10.2312/cgvc.20201150

EG UK Computer Graphics & Visual Computing (2020)
P. D. Ritsos and K. Xu (Editors)

ORQA: Objective Reflection Quality Assessment

S.G. Houwink, K.Y. Kliffen and J. Kosinka

Bernoulli Institute, University of Groningen, the Netherlands

Abstract

We present ORQA (Objective Reflection Quality Assessment), a method to objectively assess shape quality from reflection line renderings. The goal of ORQA is to correctly order existing comparable reflection line renderings according to perceived shape quality. Surface quality information is extracted from directional changes of the reflection lines. Relative importance on the directional changes and reflection line length are key aspects of scoring. ORQA is fast, stable and generalises well over various datasets.

Categories and Subject Descriptors (according to ACM CCS): I.4.7 [Image Processing and Computer Vision]: Feature Measurement—Size and Shape; Texture

1. Introduction

Different computer graphics modelling and rendering techniques, including spline and subdivision methods, generally result in surfaces of different quality. The quality is often expressed in terms of geometric continuity (G^0, G^1, and higher), which may be lower near edges and (irregular) vertices.

Reflection lines are commonly used to visualise and reveal flaws of a surface; see Fig. 1, top. Artefacts such as discontinuities, pinching effects and other irregularities are easily spotted by humans; see Fig. 1, bottom. This, however, results in subjective quality assessment. This paper presents a more objective quality assessment technique, called ORQA. It is intended for existing reflection line renderings as typically used in scientific papers [YZ04, KSD14, KP15b, BBK18, HK20], to name a few as the list is basically endless, and the car industry [Bar92, KP15a], and the field of computer aided design in general, to argue about surface quality.

The definition of reflection lines and other surface assessment techniques are described in Section 2. The computational phases of ORQA are presented in detail in Section 3. The results showing general applicability and stability of ORQA are presented in Section 4. Sections 5 and 6 are devoted to the discussion of limitations, and conclusion and future work, respectively.

2. Related work

Different definitions exist for the related concepts of reflection lines, highlight lines [BC94], and isophotes [The01]. Reflection line renderings with similar definitions can nearly always be converted to a format suitable for ORQA. In order to avoid confusion and to define relevant parameters, the following definition for reflection lines will be used. The colour of surface pixels is defined by

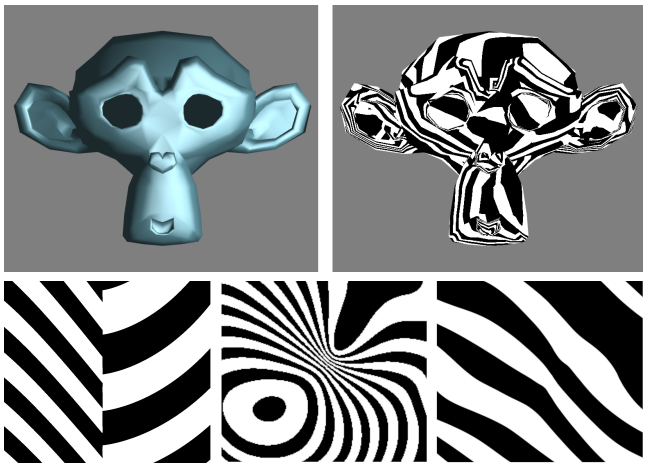

Figure 1: ***Top row****: Surface rendering (Phong shading) and reflection line rendering of Blender model Suzanne.* ***Bottom row****: Common types of reflection line rendering artefacts. From left to right are artefacts with respect to (normal) discontinuity, pinching effects, and meandering lines.*

$$\text{colour} = \begin{cases} \text{white} & \text{if } \sin\left(f\,(N\cdot C)+\phi\right) > \tau, \\ \text{black} & \text{otherwise,} \end{cases} \tag{1}$$

where f, ϕ and τ represent the reflection line frequency, phase and width, respectively, the influence of which we also study (see Fig. 8), and $N \cdot C$ is the dot product of the unit surface normal N

and a constant vector C. In this paper, $C = [1,1,1]^T$. Note that one could also use the alternative definition of using actual reflections of a surface surrounded by a spherical (or other) shape with black and white stripes on it. The concept of contour lines (or strips) [BFH86, HHS*92] or similar techniques producing lines based on surface slicing or the normal field could also be scored using ORQA.

As far as we are aware, ours is the first attempt at providing an objective scoring tool for reflection (or similar) line renderings. Although reflection (and other lines) and their curvature have been explored in the context of shape interrogation before [BC94, The95, PM09], the final scoring has, so far, relied on human assessment. An objective scorer is thus the main contribution of this paper.

3. Methodology

This section presents the methodology of ORQA in detail. But before that, we explain our high-level approach to objective scoring.

As it cannot be expected that any two (or more) reflection line renderings can be automatically compared in an objective manner (consider e.g. the last two images in the bottom row of Fig. 1), some assumptions need to be made. One such assumption is that the compared renderings use the same view (orientation, zoom, etc.) of the generated surfaces (e.g. based on quadratic vs. cubic patches) in the same position, and the reflections lines share the same parameters (frequency f, phase ϕ, width τ, and the vector C); see Eq. 1. Further, the view typically focuses on one (problematic) surface feature in the comparison. These surface features arise mainly around extraordinary vertices where the control mesh is not regular (i.e., due to the topology/connectivity of the mesh), but they can also be caused by the shape (i.e., geometry) of the mesh itself, such as at intended sharp creases.

These are natural assumptions, which are used in all high-quality publications dealing with comparing surface quality based on reflection (or similar) line renderings. On top of this, one is generally not interested in some absolute measure of quality. Instead, a relative ranking of comparable renderings, and thus spline/subdivision surface generation methods, is desired.

With these assumptions in mind, the quality assessment is performed in several phases:

- Section 3.1: Preprocessing, which may be required to transform a reflection line rendering to the desired format;
- Section 3.2: Extraction of polylines with information representative of shape quality;
- Section 3.3: Extraction of angular derivatives from the obtained polylines;
- Section 3.4: Mapping of the obtained angular derivatives to an objective score.

These stages are now described one at a time.

3.1. Preprocessing

For this purpose we used an automatic tool using random walker segmentation [Gra06] on the foreground (see Fig. 2). Only the thresholds for the markers are set manually.

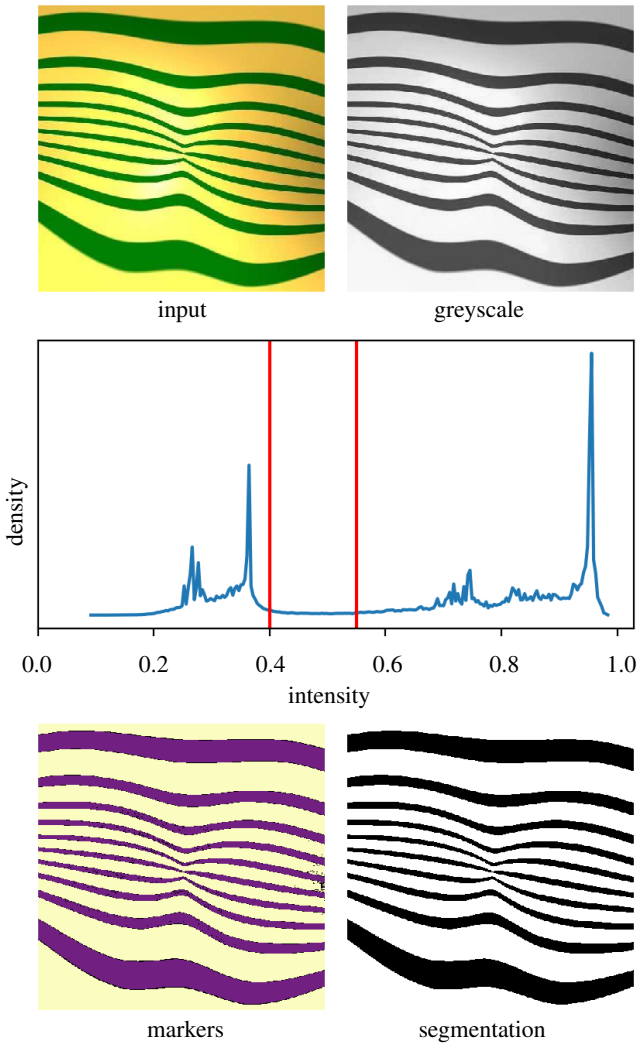

Figure 2: *Stages in preprocessing. An input image (such as this one taken from [KP18b]) is converted to grayscale, from which an intensity histogram is computed. Pixels with an intensity below 0.4 become markers for black regions, and pixels with an intensity above 0.55 become markers for white regions. The final segmentation is obtained using random walker segmentation.*

3.2. Polyline extraction

The first phase concerns the extraction of polylines representing separations between the black and white foreground regions; see Fig. 3. The marching squares algorithm having a grey level threshold anywhere between middle grey and white is used to obtain a polyline representation of the white region contours.

Sharp transitions within these polylines near foreground boundaries can in general not be considered as artefacts of the rendering method or model. Therefore, polyline segments along foreground boundaries are removed. A vertex of a polyline can be considered along the foreground boundary when its position is not contained

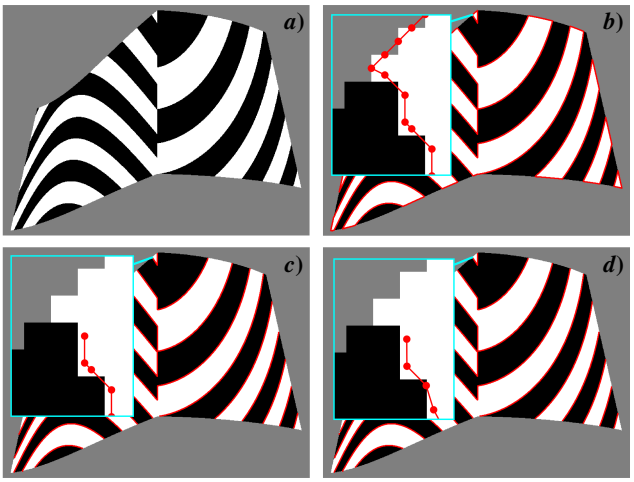

Figure 3: *Extraction of polylines representing separations between the black and white foreground regions.* ***a)*** *A reflection line rendering of two surfaces connected with a G^0 continuity.* ***b)*** *The extracted polylines for the white regions.* ***c)*** *The removed foreground boundaries.* ***d)*** *The resampled polylines.*

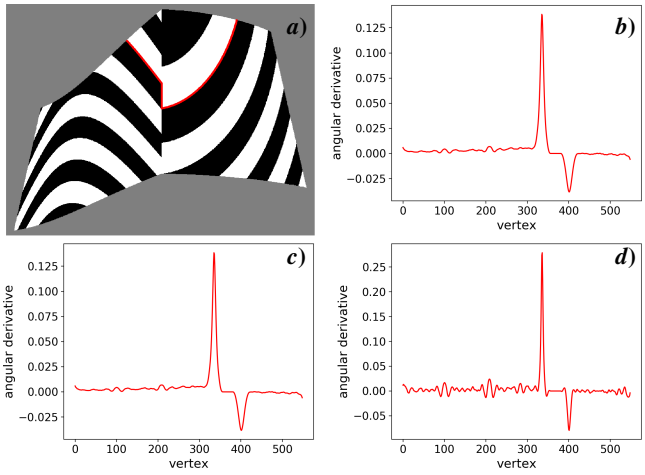

Figure 4: *The angular derivatives* ***(b)*** *obtained for the selected (red) polyline* ***(a)****. Noise comparison for linear* ***(b)****, quadratic* ***(c)****, and cubic* ***(d)*** *polynomials using the Savitzky-Golay filter.*

in the foreground morphologically eroded by a 3×3 structuring element.

The obtained polyline segments generally differ in length. In order to improve stability in further processing, they are resampled with line segments close to pixel length using linear interpolation.

3.3. Angular derivative extraction

The second phase concerns obtaining angular derivatives along the obtained polylines; see Fig. 4. The objective is to filter discretisation artefacts introduced by pixelation, while retaining artefacts introduced by the rendering method or model. Note that naïve approaches, like taking a forward difference of the angles, tend to produce noisy results.

Both dimensions of the polyline coordinates are considered as separate signals, x and y. Note that for a closed polyline the signal is considered to be wrapped, while for an open polyline the first and last element of the signal are replicated.

The angle at a polyline vertex with respect to the positive x-axis is given by

$$\theta = \operatorname{atan2}(y', x'), \tag{2}$$

and then the angular derivative at a polyline vertex is given by

$$\theta' = -\frac{y'}{x'^2 + y'^2} x'' + \frac{x'}{x'^2 + y'^2} y''. \tag{3}$$

The derivatives are obtained via the Savitzky-Golay filter [SG64], which increases data precision without distorting signal tendency. Fig. 4 indicates that a linear or quadratic fitting polynomial yields the most desirable result. We chose the linear fit for efficiency reasons in ORQA. An empirical study showed that having a filter window length of 21 offers the best trade-off between the removal of discretisation artefacts and retention of essential information for the range of rendering resolutions we considered, namely 140 to 4096 in both directions.

3.4. Scoring

The third phase concerns mapping the obtained angular derivatives to a representative score for the entire reflection line rendering. The higher the score, the lower the quality of the reflection line rendering, and thus in turn the poorer the original shape.

The first step is based on the observation that sharper transitions tend to be relatively more important compared to more moderate transitions. By raising the angular derivative θ' to some power, they are mapped to relative vertex scores. We evaluated powers between 0.5 and 3.0, and it turned out that values close to 2.0 (our default value) yield favorable results over different datasets. Note that powers greater than one essentially reduce noise as well. An initial polyline score is then obtained by summing the vertex scores corresponding to that polyline.

The second step is based on the observation that longer polylines tend to be relatively more stable and informative than shorter polylines; see Fig. 5. By multiplying the polyline scores with their respective length raised to some power, the polyline scores are mapped to relative scores. Again, we evaluated powers between 0.5 and 3.0, and also here powers close to 2.0 (our default value) yielded favorable results. The score for the entire rendering is obtained by summing the scores for all its polylines.

4. Results

We now present our results obtained with ORQA, as well as its stability and performance.

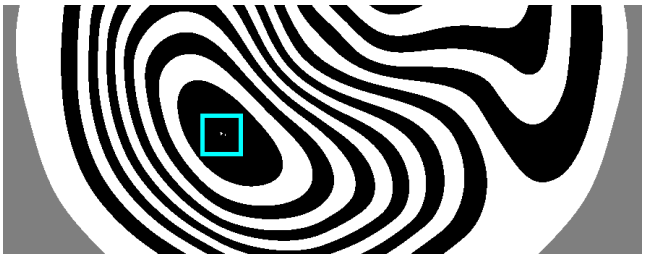

Figure 5: *Small closed contours (cyan box) are unstable with respect to phase changes. Without the relative polyline length importance, small closed polylines contribute significantly to the score, due to large angular derivatives. This effect is removed by taking into account the lengths of the polylines.*

4.1. Test cases and scores

To show the general applicability of ORQA, a varied dataset has been collected with a total of twenty-three test sets (see Figs. 9 and 10 in the Appendix). From several publications [KP15b, KP17, KP18a, KP18b, KP19, BBK18] all reflection line renderings that could be compared using ORQA, i.e., satisfying the assumptions listed in Section 3, were extracted to produce twenty test sets containing mostly two to three images each. Available reflection line methods and models produced another three test sets. For each test set, the images were labeled in decreasing order of quality based on annotations by the authors of the respective papers, considered as ground truth, and trivial observations. Resolutions ranged between 140 to 4096 pixels in both dimensions.

For 21 out of the 23 test sets all images were rated in the correct order. The renderings in Fig. 6 represent all cases for which the wrong order was produced. For the car body renderings, this can be attributed to an excessive amount of complexity and noise, as well as the relative importance on the polyline length, as the lower quality renderings contain more relatively short polylines. ORQA was not designed to handle such cases; it was designed to objectively score surface parts generated by comparable algorithms when all other parameters (view, reflection line frequency, etc.) are fixed. When used e.g. on the car hood only, it returns the expected order.

For the renderings in the right column, the wrong order can be attributed to the fact that although there is a pinch in the bottom rendering, the polylines (reflection lines) are not curved much in that region. Also note that the relative scores in this test-case are very close to each other (1.00 vs. 1.03). Further, in this and similar cases, the pinch might be actually preferred to the flat-ish spot in the shape/rendering with the worse (higher) ORQA score.

4.2. Stability

To show the stability of ORQA with respect to changes in the reflection line frequency, phase, width and resolution, several datasets have been generated having small changes in these parameters. Fig. 7 indicates that for higher values of the blending parameter p of the subdivision shading variant of [BBK18], the renderings are worse in quality. This parameter p controls the blending process in subdivision shading: lower values produce smoother results.

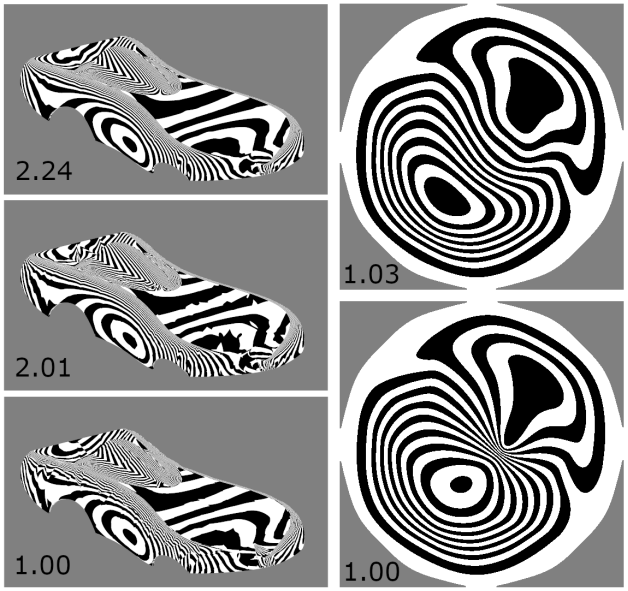

Figure 6: *The columns contain the test sets for which ORQA does not produce the correct order. The correct order in decreasing quality is from top to bottom. Note the ambiguity between the last two car body models: For the car in the middle the hood is worse, while for the car at the bottom the sides are worse. The presented scores are* relative *wrt. the best image (bottom) as judged by ORQA.*

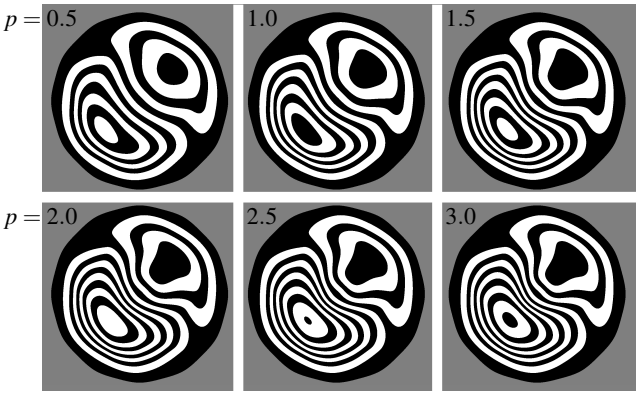

Figure 7: *The effect of varying the blending parameter p of [BBK18] between 0.5 and 3.0 for a fixed reflection line frequency, phase, width and resolution. ORQA scores these images in the correct order (see Fig. 8).*

Fig. 8 indicates that given a fixed reflection line frequency, phase, width and resolution, and a variable value of the parameter p, ORQA always produces the correct order, and can therefore be considered stable.

4.3. Performance

An average reflection line rendering with 1024 pixels in both dimensions can be fully processed in approximately 0.2 seconds us-

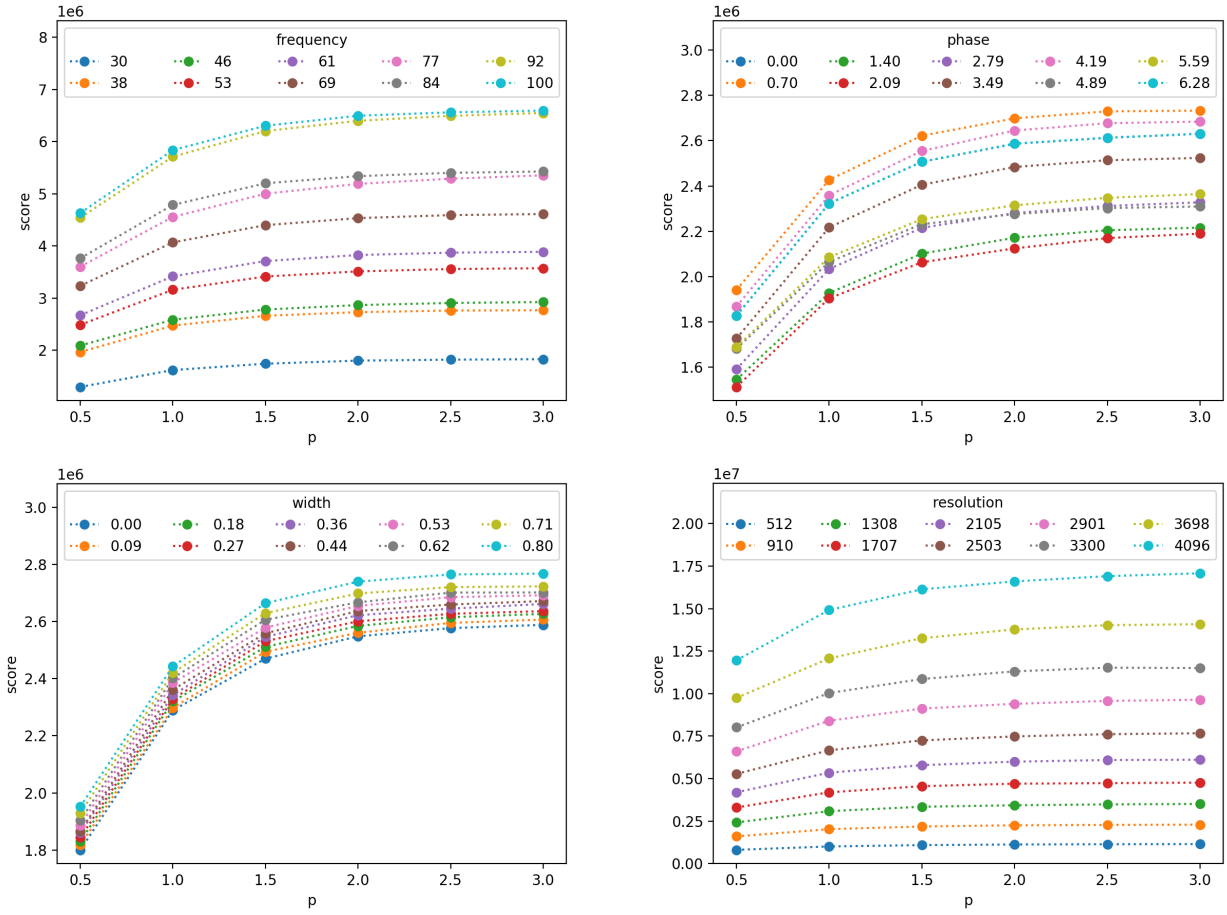

Figure 8: *Plots showing the stability of ORQA with respect to reflection line frequency, phase, width and resolution. In almost all cases, a higher value of the subdivision shading blending parameter p (all horizontal axes) results in a higher (worse) score.*

ing a serial Python implementation on a 2.8 GHz Intel Core i7 processor. Fast parallel implementations for a CPU as well as for a GPU are possible using an inherently faster programming language in combination with the embarrassingly parallel nature of the method. Consequently, quality assessment tools for rendering engines could show flaws in models in real-time by incorporating ORQA. By automatically obtaining reflection line renderings at different rotations, similar rendering techniques and models can thus be compared automatically using ORQA.

5. Discussion and Limitations

Normalisation of the score with respect to image resolution and reflection line frequency, width and phase is in some cases challenging for the following reasons. Although frequency normalisation presented promising results, in some cases an increased frequency indicates a true artefact of the rendering method which should not be normalised away. For higher resolution images actual discontinuities become relatively sharper with respect to their surroundings, and contribute relatively more to the score. This essentially improves the performance of ORQA but makes resolution normalisation challenging.

Although ORQA generalises well, it may be suboptimal in the presence of pinch artefacts which do not have substantial angular derivatives along its polylines, such as the example in Fig. 6, bottom right. Pinch artefact detectors based on reflection line density have been investigated in a hybrid setting with ORQA. This resulted in the correct ordering for some problematic test cases, but introduced wrong orderings for other test cases that showed high reflection line density that could not be considered pinch artefacts.

It has not escaped our notice that reflection lines only cover a small area of the surface compared to other methods, such as false colour mapping of mean curvature, which may provide richer information for scoring. However, as reflection line renderings are the predominant method used in the scientific and industrial literature when it comes to (subjective) shape quality assessment, we have opted for those in ORQA. This allows ORQA to be applied any future surface modelling method, but also retrospectively to results that have already appeared in the scientific literature.

6. Conclusion and Future Work

We have presented ORQA [Aut], an efficient and stable method for automatic shape quality assessment from reflection line renderings. Its key aspects are in separating discretisation noise from actual angular changes, and the relative scoring with respect to both the magnitude of angular changes and polyline lengths. We have also demonstrated the stability of ORQA with respect to variations in the parameters of the reflection line renderings.

In order to improve applicability, hybrid configurations with detectors for special types of artefacts (like pinch artefacts) require further investigation. Score normalisation, although inherently hard to achieve, might still prove useful in some applications that have to compare reflection line renderings with different frequency, phase, width or resolution. Some artefacts that are easily recognised by humans may be hard to detect directly by machines. For such cases, convolutional neural networks could be investigated as well. A potential challenge there is obtaining a large, generally applicable and ordered training dataset.

Acknowledgements This paper is based on the MSc Research Internship of the first author, which itself builds on the MSc Thesis of the second author, at the University of Groningen.

References

[Aut] AUTHORS A.: Source code. See supplementary files. 6

[Bar92] BARNHILL R. E. E.: *Geometry processing for design and manufacturing*. SIAM, Philadelphia, 1992. 1

[BBK18] BAKKER J., BARENDRECHT P., KOSINKA J.: Smooth blended subdivision shading. In *Proceedings of the 39th Annual European Association for Computer Graphics Conference: Short Papers* (2018), Eurographics Association, pp. 37–40. 1, 4

[BC94] BEIER K.-P., CHEN Y.: Highlight-line algorithm for realtime surface-quality assessment. *Computer-Aided Design 26*, 4 (1994), 268–277. 1, 2

[BFH86] BECK J., FAROUKI R., HINDS J.: Surface analysis methods. *IEEE Computer Graphics and Applications 6*, 12 (1986), 18–36. 2

[Gra06] GRADY L.: Random walks for image segmentation. *IEEE Transactions on Pattern Analysis & Machine Intelligence*, 11 (2006), 1768–1783. 2

[HHS*92] HAGEN H., HAHMANN S., SCHREIBER T., NAKAJIMA Y., WORDENWEBER B., HOLLEMANN-GRUNDSTEDT P.: Surface interrogation algorithms. *IEEE Computer Graphics and Applications 12*, 5 (1992), 53–60. 2

[HK20] HETTINGA G. J., KOSINKA J.: A multisided C^2 B-spline patch over extraordinary vertices in quadrilateral meshes. *Computer-Aided Design 127* (2020), 102855. 1

[KP15a] KARČIAUSKAS K., PETERS J.: Can bi-cubic surfaces be class A? *Computer Graphics Forum 34*, 5 (2015), 229–238. 1

[KP15b] KARČIAUSKAS K., PETERS J.: Improved shape for multi-surface blends. *Graphical models 82* (2015), 87–98. 1, 4

[KP17] KARČIAUSKAS K., PETERS J.: Improved shape for refinable surfaces with singularly parameterized irregularities. *Computer-Aided Design 90* (2017), 191–198. 4

[KP18a] KARČIAUSKAS K., PETERS J.: Rapidly contracting subdivision yields finite, effectively c2 surfaces. *Computers & Graphics 74* (2018), 182–190. 4

[KP18b] KARČIAUSKAS K., PETERS J.: Refinable bi-quartics for design and analysis. *Computer-Aided Design 102* (2018), 204–214. 2, 4

[KP19] KARČIAUSKAS K., PETERS J.: Fair free-form surfaces that are almost everywhere parametrically c2. *Journal of Computational and Applied Mathematics 349* (2019), 470–481. 4

[KSD14] KOSINKA J., SABIN M. A., DODGSON N. A.: Subdivision surfaces with creases and truncated multiple knot lines. *Computer Graphics Forum 33*, 1 (2014), 118–128. 1

[PM09] PATRIKALAKIS N. M., MAEKAWA T.: *Shape Interrogation for Computer Aided Design and Manufacturing*. Springer, 2009. 2

[SG64] SAVITZKY A., GOLAY M. J.: Smoothing and differentiation of data by simplified least squares procedures. *Analytical chemistry 36*, 8 (1964), 1627–1639. 3

[The95] THEISEL H.: *Vector Field Curvature and Applications*. PhD thesis, Universität Rostock, 1995. 2

[The01] THEISEL H.: Are isophotes and reflection lines the same? *Computer aided geometric design 18*, 7 (2001), 711–722. 1

[YZ04] YING L., ZORIN D.: A simple manifold-based construction of surfaces of arbitrary smoothness. *ACM Trans. Graph. 23*, 3 (Aug. 2004), 271–275. 1

Appendix

Figs. 9 and 10 contain our dataset, which we used to test ORQA. It has been collected from selected publications (see Section 4.1) and preprocessed (see Section 3.1), and we have rendered several test images ourselves.

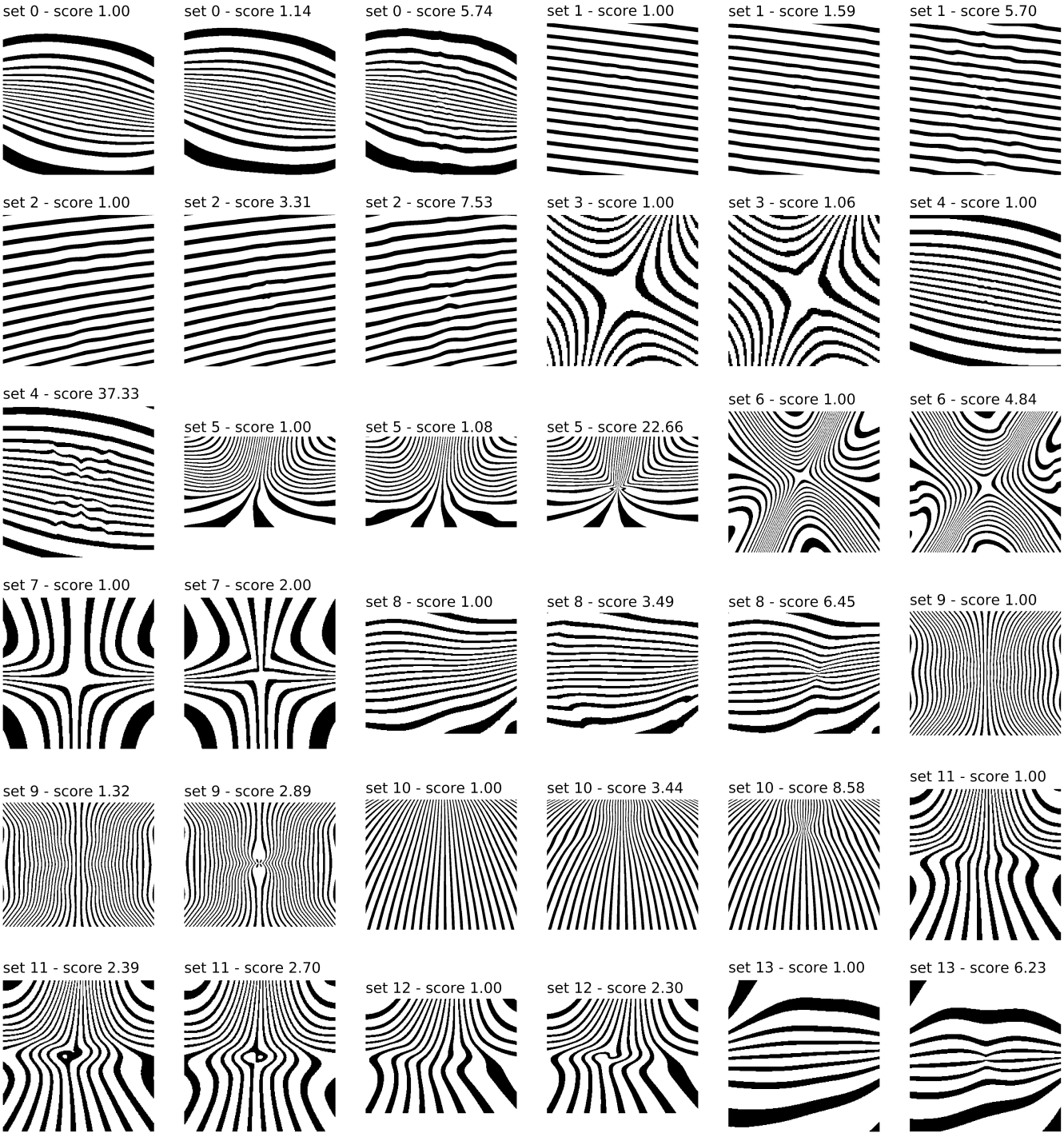

Figure 9: *The first 14 out of 23 test sets used to evaluate ORQA. The presented scores are* relative *to the score of the rendering with score 1.00 of the respective test set.*

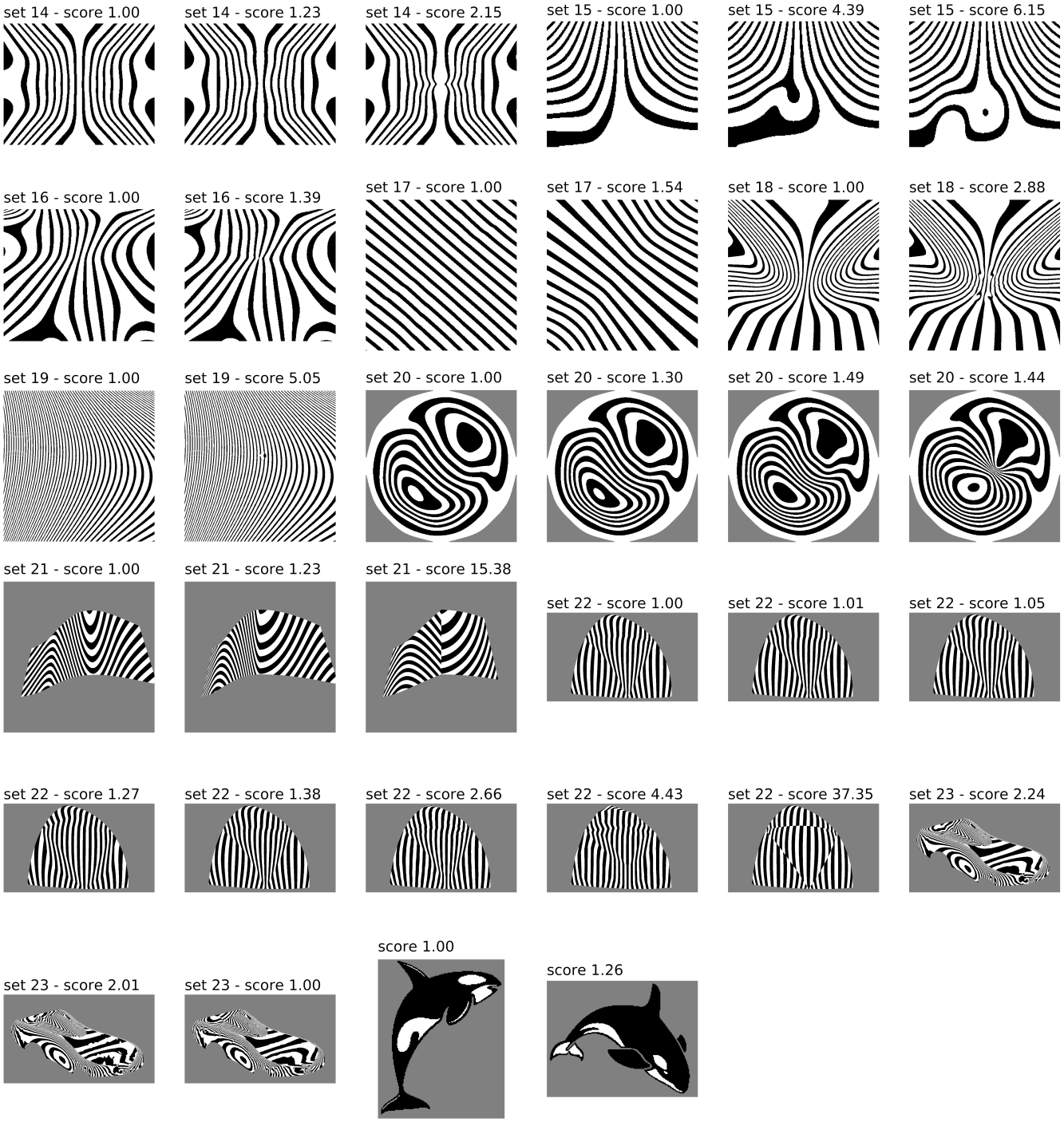

Figure 10: *The last 10 out of 23 test sets used to evaluate ORQA, plus an extra 'ORQA' pair. The presented scores are* relative *to the score of the rendering with score 1.00 of the respective test set.*